

# MRI Characteristics of Autoimmune Encephalitis With Autoantibodies to GABAA Receptor

## A Case Series

Bo Deng, MM,\* Mengfei Cai, MD,\* Yue Qiu, MD, PhD, Xiaoni Liu, MSc, Hai Yu, MM, Xiang Zhang, MD, PhD, Huifen Huang, MM, Xiuhe Zhao, MD, PhD, Wenbo Yang, MD, PhD, Siqi Dong, MB, Lei Jin, MB, Shuguang Chu, MD, PhD, and Xiangjun Chen, MD, PhD

### Correspondence

Dr. Chen  
xiangjchen@fudan.edu.cn

*Neurol Neuroimmunol Neuroinflamm* 2022;9:e1158. doi:10.1212/NXI.0000000000001158

## Abstract

### Background and Objectives

To characterize the clinical and neuroimaging phenotypes of patients with autoantibodies to  $\gamma$ -aminobutyric acid type A receptor (GABA<sub>A</sub>R).

### Methods

Ten patients with autoantibodies against GABA<sub>A</sub>R from Huashan Hospital Autoimmune Encephalitis cohort were identified. We used MRI assessments and clinical examinations to summarize major clinical profile and visualize and quantify lesion distribution features. The relationship between clinical features, neuroimaging phenotypes, and topology of GABA<sub>A</sub>R expression were further investigated.

### Results

The median age at onset of 10 patients (8 male patients and 2 female patients) with anti-GABA<sub>A</sub>R encephalitis was 41.5 years (range: 17–73 years). All patients had prominent seizures and multifocal spotted or confluent lesions involved in limbic, frontal, and temporal lobes on brain MRI. Bilateral but asymmetric lesions in cingulate gyri were observed in all patients. These involved lesions could change dynamically with immunotherapies and relapse. Distribution of patients' brain MRI lesions was positively correlated with gene expression level of  $\beta$ 3 subunit-containing GABA<sub>A</sub>R (Spearman  $\rho = 0.864$ ,  $p = 0.001$ ), the main target of autoantibodies. According to topology of lesions, patients with anti-GABA<sub>A</sub>R encephalitis could be classified into 2 clinical-radiological types: confluent type with bilateral confluent lesions involved in almost all limbic, frontal, and temporal lobes and spotted type with multiple scattered small-to-medium patchy lesions. Patients with confluent type exhibited worse clinical presentations and outcomes when compared with those with spotted type (maximum modified Rankin scale [mRS]: 5 [5–5] vs 3.5 [3–4], respectively,  $p = 0.008$ ; follow-up mRS: 4 [2–6] vs 0.5 [0–1], respectively,  $p = 0.016$ ).

### Discussion

Anti-GABA<sub>A</sub>R encephalitis has distinctive neuroimaging phenotype. Cingulate gyri were frequently involved in this disorder. The topology of lesions might be associated with the distribution of  $\beta$ 3 subunit-containing GABA<sub>A</sub>R and reflected patients' disease severity and outcomes.

\*These authors contributed equally to this work.

From the Department of Neurology (B.D., Y.Q., X.L., H.Y., X. Zhang, W.Y., S.D., L.J., X.C.), Huashan Hospital, Fudan University, Shanghai; National Center for Neurological Disorders (B.D., Y.Q., X.L., H.Y., X. Zhang, W.Y., S.D., L.J., X.C.), Shanghai, China; Department of Neurology (M.C.), Donders Institute for Brain, Cognition and Behaviour, Radboud University Medical Center, Nijmegen, the Netherlands; Institute of Neurology (X.L., X. Zhang, X.C.), Fudan University, Shanghai; Department of Neurology (H.H.), Lishui Hospital, Zhejiang University School of Medicine; Department of Neurology (X. Zhao), Qilu Hospital, Shandong University, Jinan; Department of Radiology (S.C.), Shanghai East Hospital, Tongji University School of Medicine; and Human Phenome Institute (X.C.), Fudan University, Shanghai, China.

Go to [Neurology.org/NN](https://www.neurology.org/NN) for full disclosures. Funding information is provided at the end of the article.

The Article Processing Charge was funded by the authors.

This is an open access article distributed under the terms of the Creative Commons Attribution-NonCommercial-NoDerivatives License 4.0 (CC BY-NC-ND), which permits downloading and sharing the work provided it is properly cited. The work cannot be changed in any way or used commercially without permission from the journal.

## Glossary

**AE** = autoimmune encephalitis; **AED** = antiepileptic drug; **CBA** = cell-based assay; **Caspr2** = contactin-associated protein-like 2; **FLAIR** = fluid-attenuated inversion recovery; **GABA<sub>A</sub>R** =  $\gamma$ -aminobutyric acid type A receptor; **GABA<sub>B</sub>R** =  $\gamma$ -aminobutyric acid type B receptor; **GAD** = glutamic acid decarboxylase; **HHV6** = human herpesvirus 6; **ICU** = intensive care unit; **LGI1** = leucine-rich glioma-inactivated 1; **MNI** = Montreal Neurological Institute; **MOGAD** = myelin oligodendrocyte glycoprotein-antibody-associated disease; **mRS** = modified Rankin scale; **RT** = room temperature.

Autoimmune encephalitis (AE) constitutes a large group of severe neurologic disorders associated with antibodies directed at neuronal synaptic receptors, ion channels, or cell surface proteins.<sup>1</sup> Diagnosis of AE is important because an early diagnosis and prompt treatment with immunotherapy could dramatically improve patients' outcomes.<sup>1,2</sup> Detection of autoantibodies in serum and/or CSF could confirm the diagnosis. However, it usually takes several days or weeks before obtaining antibody testing results, which might delay the diagnosis.<sup>1</sup> Moreover, many countries and regions have no access to antibody testing, especially for AE mediated by some rare antibodies. Therefore, to diagnose AE based on neuroimaging and clinical information is of great clinical significance.<sup>1</sup>

Given the broadening spectrum of clinical presentations in AE, clinical phenotypic characterization focusing on clinical and neuroimaging features could help identifying precise subtyping of AE, thus achieving an early and accurate diagnosis. For example, central hypoventilation is one of the recognizable clinical phenotypes of anti-NMDAR encephalitis.<sup>1,3</sup> More recently, comprehensive studies of leucine-rich glioma-inactivated (LGI)1 and contactin-associated protein-like (CASPR)2 antibodies-related diseases have revealed that the phenotype of faciobrachial dystonic seizures is highly specific for patients with LGI1 antibodies but not with CASPR2 antibodies.<sup>4,6</sup> These studies have shed light on how a phenotypic study could facilitate the classification and diagnosis of different subtypes of AE.

AE associated with antibodies against  $\gamma$ -aminobutyric acid type A receptor (GABA<sub>A</sub>R) is 1 recently described disease entity.<sup>7</sup> Of interest, some clinical and neuroimaging features of this disorder might make it different from other antibody-mediated encephalitis.<sup>8,9</sup> However, anti-GABA<sub>A</sub>R encephalitis is an extremely rare disease. Since the first report in 2014, only approximately 50 cases were reported worldwide.<sup>10</sup> A detailed clinical and neuroimaging description of this disorder was scarce, thus impeding an early diagnosis of this potentially treatable disorder based on disease phenotype.

In this study, we reported a case series of anti-GABA<sub>A</sub>R encephalitis in China. We investigated whether anti-GABA<sub>A</sub>R encephalitis exhibited recognizable clinical and neuroimaging phenotypes. We further examined the relationship between clinical features, neuroimaging phenotype, and gene expression pattern of GABA<sub>A</sub>R.

## Methods

### Patients

We enrolled 1,919 patients with suspected AE in Huashan Hospital, Fudan University, between January 2013 and February 2021. In 483 patients with neuronal cell surface antibodies, 10 were finally diagnosed with anti-GABA<sub>A</sub>R encephalitis. Patients' clinical information was obtained from medical records and telephone interviews. All patients had at least 1 brain MRI scan, and their images were reviewed by a neurologist (X.J.C.) and neuroradiologist (S.G.C.). We used modified Rankin scale (mRS) to evaluate the severity of symptoms at acute stage. The outcome at the last follow-up was also assessed with mRS. An outcome was considered favorable with an mRS 0–2 according to the previous study.<sup>3</sup> CT, B-mode ultrasound, or <sup>18</sup>fluorodeoxyglucose PET was performed to detect underlying tumors.

### Autoantibody Detection and Identification of Subunit-Binding Specificity With Cell-Based Assays

Previous studies demonstrated that  $\alpha$ 1,  $\beta$ 3, and  $\gamma$ 2 subunits of GABA<sub>A</sub>R were targets of autoantibodies in anti-GABA<sub>A</sub>R encephalitis.<sup>7,8,11</sup> Therefore, we first used live HEK293T cells transfected with plasmids encoding human  $\alpha$ 1 (NM\_000806.5),  $\beta$ 3 (NM\_000814.5), and  $\gamma$ 2 (NM\_198904.3) subunits of GABA<sub>A</sub>R (all were obtained from MiaoLing Plasmid Sharing Platform, Wuhan, China) in combination to screen whether patients' serum and CSF samples had autoantibodies to GABA<sub>A</sub>R. Second, when a patient's sample reacted with coexpression of  $\alpha$ 1 $\beta$ 3 $\gamma$ 2, we transfected  $\alpha$ 1,  $\beta$ 3, or  $\gamma$ 2 subunit individually to identify the subunit-binding specificity of autoantibodies from each patient. Because the  $\gamma$ 2 subunit was not well expressed in the cell surface when transfected individually, autoantibodies to  $\gamma$ 2 subunit was observed after fixation and permeabilization, as previously described.<sup>8</sup>

HEK293T cells were transfected with an equivalent amount of indicated single  $\alpha$ 1,  $\beta$ 3, or  $\gamma$ 2 subunit of GABA<sub>A</sub>R or cotransfected with 3 subunits (ratio 2:2:1). Thirty-six hours after transfection, cells were used to detect autoantibodies. For a live cell-based assay (CBA), cells were washed 3 times with phosphate-buffered saline and then incubated with serum (1:10) or CSF (1:1) for 30 minutes at room temperature (RT). Cells were washed, fixed with 4% paraformaldehyde for 5 minutes, permeabilized with 0.2% Triton X-100 for 10

minutes, and blocked with PBS containing 10% goat serum for 30 minutes at RT. For detection of autoantibodies to  $\gamma 2$  subunit, the cells were fixed, permeabilized, and blocked before incubation with a patient's serum sample. In experiments of subunit-binding specificity, cells were incubated with corresponding commercial antibodies to  $\alpha 1$  subunit (Proteintech Cat# 12410-1-AP, RRID: AB\_2108692),  $\beta 3$  subunit (Millipore Cat# MAB341, RRID: AB\_11214320), or  $\gamma 2$  subunit (Proteintech Cat# 14104-1-AP, RRID: AB\_10693527) for 2 hours at RT. Thereafter, Alexa Fluor 488-conjugated secondary antibodies and Alexa Fluor 594-conjugated secondary antibodies (1:800; Molecular probes, Eugene, OR) were applied to label human autoantibodies and commercial antibodies for 1 hour at RT. Finally, nuclei were visualized with 4',6-diamidino-2-phenylindole. Images were acquired by laser confocal scanning microscope (Olympus FV1200, Tokyo, Japan).

### Detection of Coexisting Autoantibodies

Previous studies demonstrated that patients with anti-GABA<sub>A</sub>R encephalitis could have coexisting autoantibodies.<sup>7,8,12</sup> Therefore, patients' serum and/or CSF samples were tested for onconeural antibodies (Hu, Yo, Ri, amphiphysin, CRMP5, and Tr) and antibodies to NMDAR, LGII, CASPR2,  $\alpha$ -amino-3-hydroxy-5-methyl-4-isoxazolepropionic acid receptor,  $\gamma$ -aminobutyric acid type B receptor (GABA<sub>B</sub>R) with commercially available kits (Euroimmun, Lübeck, Germany). Serum glutamic acid decarboxylase (GAD) 65 antibodies were detected with ELISA according to the manufacturer's instructions (RSR, Cardiff, United Kingdom). Only high serum level of GAD65 antibodies (>10,000 U/mL) was considered clinically relevant.

### MRI Data Acquisition

All included participants received T2-weighted fluid-attenuated inversion recovery (FLAIR) scans to identify their brain lesions. Of note, although the included participants were diagnosed in Huashan Hospital, we also retrieved these neuroimaging data from other hospitals where patients first visited at the onset of disease. Therefore, some of the participants had neuroimaging from different scanners and sequences. To visualize the lesion distribution and quantify regional volumes anatomically, we used the FLAIR scan with largest lesion volume for each case. FLAIR parameters with largest lesion volume for each case are listed in eTable 1 ([links.lww.com/NXI/A705](https://links.lww.com/NXI/A705)). All patients' lesion volumes on FLAIR scan at each time point are listed in eTable 2.

### Classifications of Lesions on FLAIR Imaging

According to the lesion patterns on FLAIR scans, we classified patients into 2 clinical-radiological types: confluent and spotted. Specifically, we semiquantitatively defined the confluent type when (1) at least half of the lesion areas grew together spanning 2 or more lobes and were not discrete with visual inspection in a consensus meeting and (2) the largest diameter of a lesion was  $\geq 3$  cm. By contrast, spotted type was primarily defined when at least half of the lesion areas were small spotted or irregular patchy lesions with scattered distribution pattern and the largest lesion diameter was <3 cm.

Besides, for patients who did not meet the criteria of confluent type, they were also defined as spotted type. Patient 2 had only head CT at acute stage, i.e., largest lesion. Because brain lesion volumes between CT and MRI scan are not easily comparable, this patient was not classified and therefore excluded when comparing clinical features, treatment, and outcome between patients in confluent type and spotted type group.

### Quantification and Probability Map of Lesions on FLAIR Imaging

To increase the accuracy of subsequent lesion segmentation, FLAIR images were first skull-stripped using brain extraction tool to remove any nonbrain tissue component.<sup>13</sup> Visible lesions on skull-stripped FLAIR scans were manually segmented by using the interactive software program ITK-SNAP,<sup>14</sup> blinded to the clinical data, followed by a consensus meeting when the disagreement occurred. A binary lesion mask for each participant was obtained.

To capture the spatial pattern of brain lesion, we generated the probabilistic lesion mapping, which is a widely used approach to visualize lesion distribution and frequency of lesion occurrence in a given brain location.<sup>15-17</sup> Because high-resolution T1-weighted scans were not available for all participants, we used the FLAIR template provided online ([brainder.org/download/flair/](http://brainder.org/download/flair/)) as the reference image to register native space FLAIR images in Montreal Neurological Institute (MNI) standard space. This nonlinear spatial normalization was performed by the `antsRegistrationSyN.sh` tool,<sup>18</sup> part of the Advanced Normalization Tools software package ([stnava.github.io/ANTS/](https://github.com/stnava/ANTS)). First, we registered binarized lesion masks in MNI space for each patient. Probabilistic lesion mapping was generated by first merging and then averaging all the lesion masks onto MNI template, and it indicated the percentage of patients who had lesions localized in a certain brain region. The registration results were visually inspected, and manual adjustments were made in case of minor displacements.

### GABA<sub>A</sub>R Gene Expression Data and Brain Lesion Analysis

Previous studies demonstrated patients' autoantibodies could bind to  $\alpha 1$ ,  $\beta 3$ , or  $\gamma 2$  subunit of GABA<sub>A</sub>R, but  $\beta 3$  subunit was the most frequent subunit that could be recognized by autoantibodies.<sup>8</sup> We hypothesized that the distribution of patients' MRI lesions could be related to the topology of GABA<sub>A</sub>R expression across the brain. Therefore, we first visualized the gene expression level of  $\alpha 1$ ,  $\beta 3$ , and  $\gamma 2$  subunits (*GABRA1*, *GABRB3*, and *GABRG2*), as previously described.<sup>19</sup> In brief, complete microarray gene expression data sets were downloaded from the Allen Institute of Brain ([human.brain-map.org/static/download](http://human.brain-map.org/static/download)).<sup>20</sup> These data were originally obtained from 6 individuals. Gene expression was assayed by the Allen Institute with custom-designed Agilent arrays. Block-face images of tissue slabs were used to map samples of gene expression to anatomical locations. Before brain dissection, whole brain MRI images were obtained for each brain. The

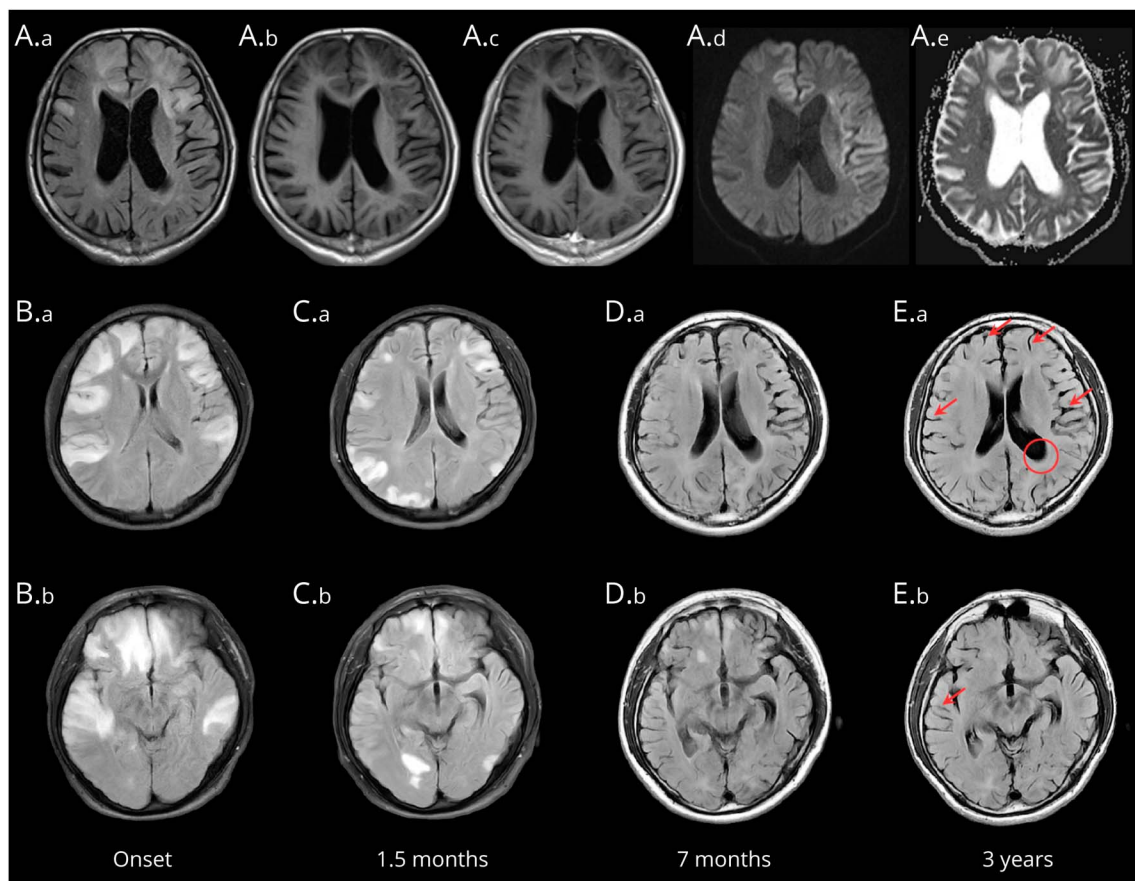
**Table 1** Demographics, Clinical Profiles, and Auxiliary Examinations of Anti-GABA<sub>A</sub>R Encephalitis Cases

Patient no.	Age/sex	Prodromal symptoms	Onset symptom	Main clinical symptoms	Maximum mRS	ICU admission	Types of brain MRI <sup>a</sup>	GABA <sub>A</sub> R subunit-binding specificity	CSF	EEG
1	17/M	Fever	Memory impairment	FS, GS, SE, cognitive deficits, irritability, psychosis, movement disorder, speech dysfunction, hearing loss, weakness and numbness in right limbs, and coma	5	Yes	Type 1	α1, β3, γ2	Elevated protein	Diffuse slowing, bilateral with R-dominant epileptiform activity
2	29/M	Excessive sweating, malaise	Seizure	FS, GS, SE, cognitive deficits, irritability, mood and behavioral change, speech dysfunction, autonomic dysfunction, muscle cramps, and coma	5	Yes	NA <sup>b</sup>	α1, β3	Normal	Bilateral with R-dominant slowing and epileptiform activity
3	68/M	None	Memory impairment	FS, GS, SE, cognitive deficits, psychosis, and coma	5	Yes	Type 1	α1, β3	Normal	Diffuse slowing, bilateral epileptiform activity
4	73/M	None	Seizure	FS, GS, SE, cognitive deficits, irritability, psychosis, movement disorder, and coma	5	Yes	Type 1	α1, β3	Elevated protein, OCBs	Bilateral with L-dominant frontal focal slowing and epileptiform activity
5	57/F	HHV6 encephalitis	Seizure	FS, GS, SE, cognitive deficits, hallucinations, and coma	5	Yes	Type 1	α1, β3	Normal	Diffuse slowing and bilateral PED
6	66/M	None	Confusion	FS, GS, SE, cognitive deficits, confusion, hallucinations, personality change, sleep disorder, speech dysfunction, and coma	5	Yes	Type 1	α1, β3	Normal	Diffuse slowing and bilateral epileptiform activity
7	45/M	None	Seizure	FS, GS, cognitive deficits, emotional instability, and behavioral change	3	No	Type 2	α1, β3	Elevated protein	R hemisphere slowing and epileptiform activity
8	29/F	Headache, fever, and vomiting	Seizure	FS, GS, SE, cognitive deficits, apathy, behavioral change, speech dysfunction, right arm movement disorder, sleep disorder, and confusion	4	No	Type 2	α1, β3	Pleiocytosis	L PED and diffuse slowing
9	38/M	Headache	Memory impairment, and confusion	FS, GS, SE, cognitive deficits, confusion, irritability, bizarre behavior, movement disorder, and speech dysfunction	4	No	Type 2	α1, β3	Elevated protein	Bilateral slowing and epileptiform activity
10	24/M	None	Seizure	FS, GS, cognitive deficits, irritability, behavioral change, and dysgeusia	3	No	Type 2	α1, β3, γ2	Normal	Diffuse slowing

Abbreviations: FS = focal seizure; GABA<sub>A</sub>R = γ-aminobutyric acid type A receptor; GS = generalized seizure; HHV6 = human herpesvirus 6; ICU = intensive care unit; mRS = modified Rankin scale; NA = not available; OCB = oligoclonal band; PED = periodic epileptiform discharges; SE = status epilepticus.

<sup>a</sup> According to the extent of lesions, brain MRI of patients were classified into 2 types: confluent type (type 1) and spotted type (type 2).

<sup>b</sup> Patient 2 was not classified because of lack of head MRI at acute stage, i.e., largest lesion.



Note that multiple cortical and subcortical lesions show hyperintense signal on FLAIR imaging (A.a), hypointense signal on T1-weighted imaging without evident mass effect and gadolinium enhancement (A.b, A.c), and no significant restricted diffusion on diffusion-weighted imaging and apparent diffusion coefficient maps (A.d, A.e). Long-term follow-up FLAIR scans in 1 representative patient (patient 1) show confluent lesions predominantly involved bilateral frontal and temporal lobes at the acute stage (B.a, B.b). Some lesions disappeared, but new multifocal lesions emerged 1.5 months later (C.a, C.b). Seven months after onset, most intracranial lesions at acute stage resolved, but signs of cortical atrophy and enlarged lateral ventricles appeared (D.a, D.b). Three years after onset, this patient had stable clinical symptoms without any lesion but dilated lateral ventricles (red circle) and brain atrophy predominantly involved in temporal and frontal lobes (red arrow) (E.a, E.b). Of note, the FLAIR scans at the follow-ups were registered in the native FLAIR space at baseline to ensure that the scans from 4 time points were comparable anatomically with a side-by-side inspection. FLAIR = fluid-attenuated inversion recovery; GABA<sub>A</sub>R =  $\gamma$ -aminobutyric acid type A receptor.

MRI images were registered to the MNI152 space using FreeSurfer (help.brain-map.org/display/humanbrain/Documentation).<sup>20</sup> The downloaded raw data (expression values and the MNI152 X, Y, and Z coordinates for each brain location) were processed with data reduction steps and further mapped into FreeSurfer space from MNI152 space. Last, values of gene expression were averaged across all voxels mapped into the Desikan-Killiany cortical atlas built into the FreeSurfer software for automatic labeling of regions of interest. These steps have been constructed into a fully established pipeline by French et al.<sup>19</sup> They offered an R script to convert the gene expression data into 3D images. This script produces a gene-specific color lookup table for the FreeSurfer annotation files.

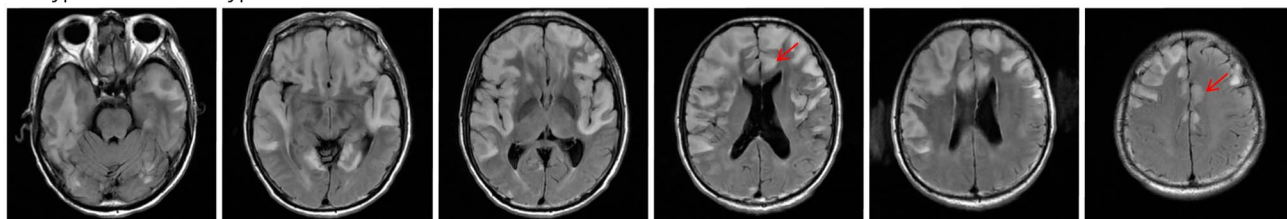
Moreover, the correlation between patients' distribution of lesions and brain regional gene expression level was investigated, as previously described.<sup>21</sup> In brief, gene expression levels of  $\alpha 1$ ,  $\beta 3$ , and  $\gamma 2$  subunits, which were expressed as  $z$

scores, were downloaded from the Allen Institute of Brain.<sup>20</sup> The mean expression levels of 3 subunits in the limbic lobe, frontal lobe, temporal lobe, insular lobe, parietal lobe, occipital lobe, basal ganglia, thalamus, cerebellum, and brainstem were calculated. The proportions of patients who had lesions fell into these anatomical regions were also calculated. Finally, the relationship between gene expression level and proportion of patients who had MRI lesions in these brain regions was analyzed by the Spearman correlation analysis.

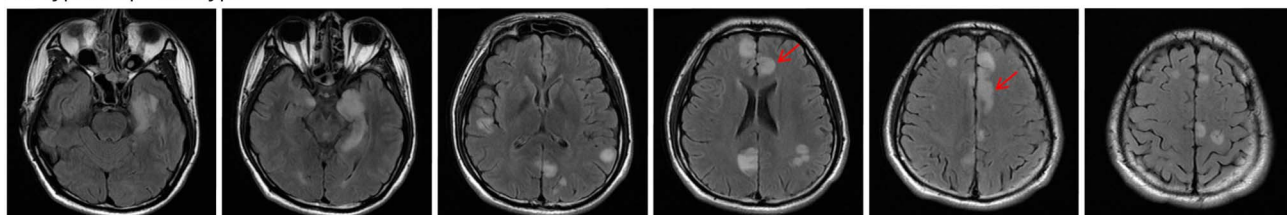
### Statistical Analysis

Statistical analysis was performed with SPSS software, version 20 (IBM, Chicago, IL) and GraphPad Prism, version 6 (GraphPad Software, San Diego, CA). Data were presented as mean  $\pm$  SD for normal distribution data and median (range) for non-normal distribution data. Normal distribution data were compared by the Student *t* test, and nonnormal distribution data were compared by Mann-Whitney *U* test. We used the Spearman correlation to examine the correlation

A. Type 1: Confluent type



B. Type 2: Spotted type



Type 1: confluent type (A); type 2: spotted type (B). Note that patients with both types had bilateral but asymmetric lesion involvement in cingulate gyri (red arrow). GABA<sub>A</sub>R =  $\gamma$ -aminobutyric acid type A receptor.

between gene expression level and distribution of MRI lesions. A 2-tailed  $p < 0.05$  was considered as statistical significance.

### Standard Protocol Approvals, Registrations, and Patient Consents

This study was approved by the institutional review board of Huashan Hospital, Fudan University. Written informed consent was obtained from each participant.

### Data Availability

Anonymized data are available on reasonable request from any qualified investigator.

## Results

### Clinical Characteristics

We identified 10 patients (age 17–73 years, median 41.5 years; 8 male patients and 2 female patients) with anti-GABA<sub>A</sub>R encephalitis from Huashan Hospital Autoimmune Encephalitis cohort (Table 1). GABA<sub>A</sub>R autoantibodies were detected in both serum and CSF samples from all patients. Representative live CBAs of patients' samples are shown in eFigure 1 ([links.lww.com/NXI/A705](https://links.lww.com/NXI/A705)). The flow diagram of diagnostic process is shown in eFigure 2.

Seizures were the dominant neurologic symptoms at the onset, which occurred in 6 patients. All patients experienced both focal and generalized convulsive seizures. Eight patients experienced status epilepticus. Six patients were admitted to intensive care unit (ICU) because of uncontrolled seizures. All patients also had cognitive deficits and psychiatric symptoms during the clinical course. Other clinical manifestations included decreased level of consciousness (8/10), speech dysfunction (5/10), movement disorder (4/10), sleep

disorder (2/10), autonomic dysfunction (1/10), and peripheral nerve hyperexcitability (1/10). Demographics and clinical features of patients are summarized in Table 1.

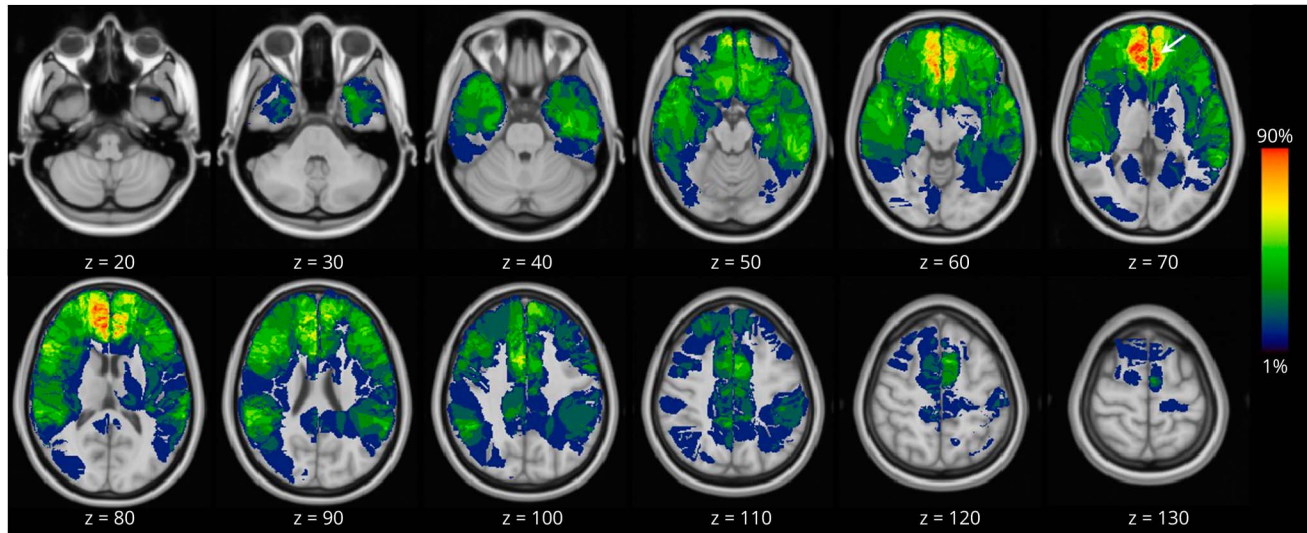
### Neuroimaging Findings

All patients presented with remarkable multiple or confluent cortical and subcortical lesions on T2-FLAIR imaging without evident mass effect, gadolinium enhancement, and restricted diffusion (Figure 1). No evidence of lactate accumulation or increased ratios of N-acetyl aspartate to choline is shown on proton magnetic resonance spectroscopy (data not shown).

According to the topology of lesions on FLAIR scans, we classified patients into 2 clinical-radiological types: confluent and spotted types. The confluent type was characterized by bilateral frontal, temporal, and limbic confluent lesion distribution and identified in 5 patients; whereas spotted type (in 4 patients) comprised multiple scattered small spotted or irregular patchy lesions. We quantified largest lesion volumes for each patient (except for patient 2) and found the mean lesion volume in confluent type group was much larger compared with that in the spotted lesion group ( $313 \pm 114 \text{ cm}^3$  vs  $80 \pm 19 \text{ cm}^3$ ,  $p = 0.005$ ). Representative brain MRI scans of 2 types are shown in Figure 2. Compared with spotted type, patients with confluent type had more severe disease, reflected by maximum mRS (5 [5–5] vs 3.5 [3–4],  $p = 0.008$ ) and a higher rate of ICU admission (100% vs 0).

In our series, patients' brain lesions frequently appeared in the limbic lobe (10/10), frontal lobe (10/10), and temporal lobe (10/10), but no patient had lesion in the cerebellum and brainstem (0/10) (eFigure 3, [links.lww.com/NXI/A705](https://links.lww.com/NXI/A705)). Lesion probability map also revealed that all lesions were distributed in supratentorial region but not likely in

**Figure 3** Lesion Probability Map of Anti-GABA<sub>A</sub>R Encephalitis



Note that limbic (especially bilateral anterior cingulate gyri, white arrow), frontal, and temporal lobes were dominantly involved. GABA<sub>A</sub>R =  $\gamma$ -aminobutyric acid type A receptor.

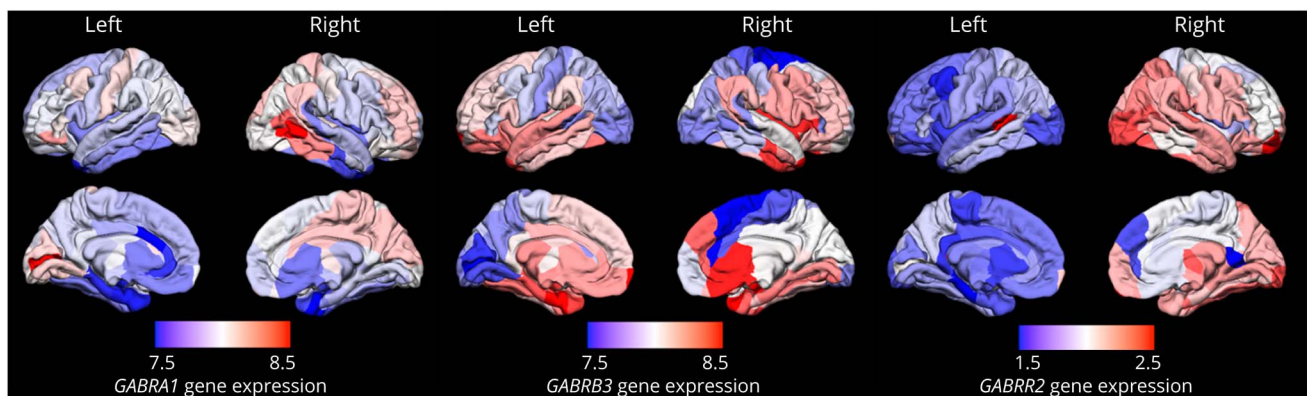
infratentorial regions (Figure 3). Of interest, all patients were featured by bilateral but asymmetric cingulate gyri involvement (Figures 2 and 3).

Autoantibodies from all 10 patients in our cohort reacted to  $\alpha 1$  and  $\beta 3$  subunits but only 2 reacted to  $\gamma 2$  subunit (Table 1 and eFigure 4, [links.lww.com/NXI/A705](https://links.lww.com/NXI/A705)). To explore whether the distinctive distribution of MRI lesions in anti-GABA<sub>A</sub>R encephalitis is related to the expression level of GABA<sub>A</sub>R (especially  $\beta 3$  subunit), we first visualized gene expressions of  $\alpha 1$ ,  $\beta 3$ , and  $\gamma 2$  subunits projected onto the FreeSurfer cortical regions. These results demonstrated that  $\beta 3$  subunit, but not  $\alpha 1$  or  $\gamma 2$  subunit, was highly expressed in

limbic, frontal, and temporal lobes (Figure 4). We also found  $z$  scored mean expression of  $\beta 3$  subunit gene (*GABRB3*) in supratentorial region ( $0.81 \pm 0.45$ ) was higher than that in infratentorial region ( $-0.74 \pm 0.57$ ) ( $p < 0.001$ ). Meanwhile, a positive correlation was demonstrated between the expression level of *GABRB3* and distribution of MRI lesions of 10 patients in each brain region (Spearman  $\rho = 0.864$ ,  $p = 0.001$ ). However, neither  $\alpha 1$  nor  $\gamma 2$  subunit expression level was correlated with the topology of MRI lesions ( $\alpha 1$ : Spearman  $\rho = 0.342$ ,  $p = 0.334$ ;  $\gamma 2$ : Spearman  $\rho = -0.565$ ,  $p = 0.089$ ).

Of interest, follow-up FLAIR scans demonstrated that the brain lesions of patient dynamically changed during the

**Figure 4** Lateral and Medial Views of *GABRA1*, *GABRB3*, and *GABRR2* Gene Expression Data Projected Onto the FreeSurfer Cortical Regions



Expression level was log<sub>2</sub> transformed. Note the high expression of *GABRB3* in limbic, frontal, and temporal lobes but a relative low expression in parietal and occipital lobes.

**Table 2** Immunologic Features, Treatment, and Outcomes of Anti-GABA<sub>A</sub>R Encephalitis Patients

Patient no.	Additional antibodies	Tumor	Relapse	Interval from onset to immunotherapy, d	First-line treatment	AEDs	Second-line treatment	Last follow-up, mo; mRS
1	None	None	Yes	41	HDMP	VPA, CBZ, LEV, TPM, DZP, PB, CZP	No	89; 2
2	LG11, <sup>a</sup> Caspr2, <sup>a</sup> GAD <sup>b</sup>	Thymoma	Yes	7	HDMP, IVIG, PE	VPA, LEV	RTX, CTX	54; 2
3	None	None	No	32	PE, IVIG	VPA, CBZ, OXC, LEV, TPM, DZP, PB, LTG	No	36; 4
4	LG11 <sup>c</sup>	None	No	67	PE, IVIG	VPA, DZP, LEV	No	7; 6
5	None	None	No	4	HDMP, IVIG, PE	VPA, CZP, LEV, LTG, TPM	No	7; 6
6	None	None	No	9	HDMP, IVIG, PE	OXC, LEV, MDZ	No	3; 3
7	None	Thymoma	No	20	HDMP	VPA, LEV	MMF	99; 0
8	None	None	Yes	6	HDMP, IVIG	VPA, OXC, LEV, CZP, MDZ	No	18; 1
9	GAD <sup>b</sup>	None	No	9	HDMP, IVIG	VPA, LEV	No	17; 0
10	None	Thymoma	No	54	HDMP	VPA, CBZ	No	2; 1

Abbreviations: AED = antiepileptic drug; AZA = azathioprine; Caspr2 = contactin-associated protein-like 2; CBA = cell-based assay; CBZ = carbamazepine; CTX = cyclophosphamide; CZP = clonazepam; DZP = diazepam; GABA<sub>A</sub>R =  $\gamma$ -aminobutyric acid type A receptor; GAD = glutamic acid decarboxylase; HDMP = high-dose methylprednisolone; IVIG = IV immunoglobulin; LEV = levetiracetam; LG11 = leucine-rich glioma-inactivated 1; MDZ = midazolam; MMF = mycophenolate mofetil; mRS = modified Rankin scale; OXC = oxcarbazepine; PB = phenobarbital; PE = plasma exchange; RTX = rituximab; TPM = topiramate; VPA = valproate.

<sup>a</sup> LG11 and Caspr2 antibodies showed positive results in serum and negative results in CSF by CBAs.

<sup>b</sup> The GAD65 antibody titers of both patients were higher than 10,000 U/mL by ELISA.

<sup>c</sup> LG11 antibodies were tested positive both in serum and CSF by CBA.

clinical course. In short-term follow-up (e.g., usually within 6 months after onset), some lesions diminished or disappeared, but some lesions could enlarge or new lesions could appear at the same time, although patients' clinical status was stable or improved after treatment. In long-term follow-up (e.g., over 1 year after onset), brain lesions usually disappeared with clinical improvement. In 3 patients with relapses, new lesions always appeared in different brain regions. Long-term follow-up FLAIR scans (in 2 patients) at 3 and 4 years showed cortical atrophy and enlarged lateral ventricle. Representative follow-up scans are shown in Figure 1.

### Treatment and Outcome

All patients received immunotherapies, of whom 7 had at least 2 kinds of first-line immunotherapeutic agents, whereas 2 received second-line immunotherapeutic agents. All patients received prescription with multiple antiepileptic drugs (AEDs). Notably, when immunotherapies were given to patients, seizures became controllable with reduced dosage of AEDs. The median follow-up time was 17.5 months (range 2–99 months). Eight patients became seizure free with oral AEDs at the last follow-up. Among 6 patients achieving favorable outcome, 4 had spotted lesion type. Two patients with confluent lesion type deceased, 1 died of severe pulmonary infection and the other died of complications of disseminated intravascular coagulation. Age, interval from disease onset to immunotherapy, proportion of underlying tumor, and follow-up time were not significantly different between patients in confluent type and

spotted type group (all  $p > 0.05$ ). However, patients with confluent type had poorer outcome than patients with spotted type (mRS: 4 [2–6] vs 0.5 [0–1],  $p = 0.016$ ). Detailed treatment and outcome data are summarized in Table 2.

## Discussion

AE associated with antibodies against GABA<sub>A</sub>R was first described in 2014.<sup>7</sup> In this study, we identified 10 patients with anti-GABA<sub>A</sub>R encephalitis with a detailed description of clinical and neuroimaging phenotypes, thus providing a better understanding of this disorder: (1) Lesions in patients with anti-GABA<sub>A</sub>R encephalitis had the dominant predilection site in supratentorial regions (i.e., limbic, frontal, and temporal), and lesion involvement in bilateral cingulate gyri was observed in all patients. This distinctive lesion distribution pattern could be positively associated with the expression level of  $\beta 3$  subunit-containing GABA<sub>A</sub>R. (2) Anti-GABA<sub>A</sub>R encephalitis could be classified into 2 topological types, namely confluent type and spotted type. Patients with confluent type had worse clinical course and poorer outcomes. (3) On temporal evolution, brain lesions of anti-GABA<sub>A</sub>R encephalitis were dynamic during the clinical course, with diminishment after immunotherapies and new lesions during relapse.

In clinical practice, multifocal brain lesions in MRI could be caused by a variety of underlying etiologies, such as tumors,



demyelinating diseases, infections, and mitochondrial encephalomyopathy, lactic acidosis, and stroke-like episodes. As a consequence, correct differential diagnosis is challenging. Our study validated that multifocal cortical-subcortical MRI abnormalities were the core imaging features of anti-GABA<sub>A</sub>R encephalitis.<sup>7,8</sup> In fact, all patients in our study and most cases in previous reports presented with multifocal or confluent lesions on brain MRI.<sup>10</sup> Therefore, anti-GABA<sub>A</sub>R encephalitis should be considered as a possible etiology for this condition. By extensively reviewing cases from previous studies<sup>7-9,22,23</sup> and quantitative analysis of lesions in our series, 3 distinctive imaging features of anti-GABA<sub>A</sub>R encephalitis could be summarized. First, lesions of anti-GABA<sub>A</sub>R encephalitis presented without mass effect, enhancement, or restricted diffusion. Second, these lesions were mainly distributed in supratentorial regions, and the predilection regions were limbic, frontal, and temporal lobes. Third, lesion in bilateral cingulate gyri could be a recognizable feature of anti-GABA<sub>A</sub>R encephalitis because this sign was presented in all patients of this study and cases from previous reports.<sup>7-9,22,23</sup> To the best of our knowledge, only 3 reported cases of myelin oligodendrocyte glycoprotein antibody-associated disease (MOGAD) showed similar lesions in cingulate gyrus.<sup>24,25</sup> However, lesions in anti-GABA<sub>A</sub>R encephalitis had asymmetric distribution, more frequently involved in anterior cingulate gyrus, still making it different from MOGAD. In summary, the above-mentioned neuroimaging phenotype was a strong indicator of anti-GABA<sub>A</sub>R encephalitis, which could be useful to distinguish this disorder from other mimics.

In view of our findings, it would be intuitive to raise the question about why anti-GABA<sub>A</sub>R encephalitis presented a distinctive lesion distribution pattern. Therefore, we explore whether this phenomenon is related to the topology of GABA<sub>A</sub>R expression. Indeed, our study found that in supratentorial regions where there were multiple brain MRI lesions, the mean *z* scored *GABRB3* gene expression level was much higher compared with that in the infratentorial region (no MRI lesion). Moreover, the expression level of  $\beta 3$  subunit, but not  $\alpha 1$  or  $\gamma 2$  subunit, was positively correlated with the distribution of brain MRI lesions of patients. Subunit-binding specificity studies of previous reported cases<sup>7,8,12</sup> and our cases demonstrated that 92.1% (35/38), 81.6% (31/38), and 28.9% (11/38) of the patients with anti-GABA<sub>A</sub>R encephalitis had autoantibodies reacted to  $\beta 3$ ,  $\alpha 1$ , and  $\gamma 2$  subunit, respectively (eFigure 5, [links.lww.com/NXI/A705](https://links.lww.com/NXI/A705)), indicating  $\beta 3$  subunit was the main subunit that could be recognized by autoantibodies of patients. This result further corroborated the close relationship between  $\beta 3$  subunit expression, autoantibody-binding preference, and MRI lesion distribution. Of interest, a trend of negative correlation between expression level of  $\gamma 2$  subunit and patients' distribution of lesions was found (Spearman  $\rho = -0.565$ ,  $p = 0.089$ ), suggesting that lower  $\gamma 2$  subunit expression might correlate with lesion burden. However, this finding from our study was limited by small sample size. Future larger studies are warranted to confirm this observation. Taken together, our study demonstrated that cerebral lesion distribution pattern in anti-GABA<sub>A</sub>R encephalitis could reflect

the topology of  $\beta 3$  subunit-containing GABA<sub>A</sub>R, thus providing a new insight into the distinctive lesion features of this disorder.

Five patients in our series showed extensive confluent lesions spanning 2 or more lobes. These patients had prominent seizures and decreased consciousness and needed an ICU admission. We classified these patients into confluent type group. However, the other 4 patients with multiple scattered spotted or patchy lesions had less severe symptoms and did not need an ICU admission. These patients were classified into spotted type group. In the long-term follow-up, patients with confluent type had poorer outcomes as well. Therefore, the extent of brain MRI lesions could be a potential useful marker of disease severity and prognosis. In light of the relationship between MRI lesion distribution, the topology of  $\beta 3$  subunit-containing GABA<sub>A</sub>R, vanishing of lesions after immunotherapies, and emergence of new lesions at relapse, we considered  $\beta 3$  subunit-containing GABA<sub>A</sub>R might be dominantly affected in this disorder. Previous studies have found that autoantibodies could reduce the number of synaptic  $\beta 3$  subunit-containing GABA<sub>A</sub>R clusters and decrease the current mediated by GABA<sub>A</sub>R in cultured hippocampal neurons.<sup>7,12</sup> However, further studies are warranted to clarify the relationship between the pathogenic effects of autoantibodies and imaging phenotype of multiple brain lesions and whether the extent of brain lesions could reflect the intensity of antibody-mediated pathogenic reaction.

Our study had several limitations. First, this was a retrospective, single-center study with relatively small sample size. Multivariable analysis or stratified analysis to identify possible confounders is confined by sample size. Further studies, preferably with larger sample size, are needed to validate the relationship between 2 types of MRI lesions and clinical outcomes. Second, we did not include children and could not compare the phenotypic difference between children and adults. Third, we did not quantify brain atrophy due to the lack of high-resolution T1 scans. High-resolution MRI data and advanced imaging techniques are needed to further elucidate the specific abnormal imaging phenotype and its association with clinical findings.

## Study Funding

This study was supported by the grants from the Clinical Research Plan of SHDC (No. SHDC2020CR2027B) and 2020 Central Transfer Payment Medical Siege Institutions Capacity Building Project (National and Provincial Multiscientific Cooperation Diagnosis and Treatment of Major Diseases Capacity Building Project).

## Disclosure

The authors report no disclosures relevant to the manuscript. Go to [Neurology.org/NN](https://Neurology.org/NN) for full disclosures.

## Publication History

Received by *Neurology: Neuroimmunology & Neuroinflammation* September 7, 2021. Accepted in final form February 7, 2022. Submitted and externally peer reviewed. The handling editor was Josep O. Dalmau, MD, PhD, FAAN.

## Appendix Authors

Name	Location	Contribution
<b>Bo Deng, MM</b>	Department of Neurology, Huashan Hospital, Fudan University, Shanghai; National Center for Neurological Disorders, Shanghai, China	Drafting/revision of the article for content, including medical writing for content; major role in the acquisition of data; and analysis or interpretation of data
<b>Mengfei Cai, MD</b>	Department of Neurology, Donders Institute for Brain, Cognition and Behaviour, Radboud University Medical Center, Nijmegen, the Netherlands	Drafting/revision of the article for content, including medical writing for content, and analysis or interpretation of data
<b>Yue Qiu, MD, PhD</b>	Department of Neurology, Huashan Hospital, Fudan University, Shanghai; National Center for Neurological Disorders, Shanghai, China	Major role in the acquisition of data; analysis or interpretation of data
<b>Xiaoni Liu, MSc</b>	Department of Neurology, Huashan Hospital, Fudan University, Shanghai; National Center for Neurological Disorders, Shanghai; Institute of Neurology, Fudan University, Shanghai, China	Major role in the acquisition of data and analysis or interpretation of data
<b>Hai Yu, MM</b>	Department of Neurology, Huashan Hospital, Fudan University, Shanghai; National Center for Neurological Disorders, Shanghai, China	Major role in the acquisition of data and analysis or interpretation of data
<b>Xiang Zhang, MD, PhD</b>	Department of Neurology, Huashan Hospital, Fudan University, Shanghai; National Center for Neurological Disorders, Shanghai; Institute of Neurology, Fudan University, Shanghai, China	Major role in the acquisition of data and analysis or interpretation of data
<b>Huifen Huang, MM</b>	Department of Neurology, Lishui Hospital, Zhejiang University School of Medicine, China	Major role in the acquisition of data and analysis or interpretation of data
<b>Xiuhue Zhao, MD, PhD</b>	Department of Neurology, Qilu Hospital, Shandong University, Jinan, China	Major role in the acquisition of data; analysis or interpretation of data
<b>Wenbo Yang, MD, PhD</b>	Department of Neurology, Huashan Hospital, Fudan University, Shanghai; National Center for Neurological Disorders, Shanghai, China	Major role in the acquisition of data and analysis or interpretation of data
<b>Siqi Dong, MD</b>	Department of Neurology, Huashan Hospital, Fudan University, Shanghai; National Center for Neurological Disorders, Shanghai, China	Major role in the acquisition of data and analysis or interpretation of data
<b>Lei Jin, MB</b>	Department of Neurology, Huashan Hospital, Fudan University, Shanghai; National Center for Neurological Disorders, Shanghai, China	Major role in the acquisition of data and analysis or interpretation of data
<b>Shuguang Chu, MD, PhD</b>	Department of Radiology, Shanghai East Hospital, Tongji University School of Medicine, China	Drafting/revision of the article for content, including medical writing for content; study concept or design; and analysis or interpretation of data

## Appendix (continued)

Name	Location	Contribution
<b>Xiangjun Chen, MD, PhD</b>	Department of Neurology, Huashan Hospital, Fudan University, Shanghai; National Center for Neurological Disorders, Shanghai; Institute of Neurology, Fudan University, Shanghai; Human Phenome Institute, Fudan University, Shanghai, China	Drafting/revision of the article for content, including medical writing for content; study concept or design; and analysis or interpretation of data

## References

- Graus F, Titulaer MJ, Balu R, et al. A clinical approach to diagnosis of autoimmune encephalitis. *Lancet Neurol*. 2016;15(4):391-404.
- Dalmau J, Graus F. Antibody-mediated encephalitis. *N Engl J Med*. 2018;378(9):840-851.
- Titulaer MJ, McCracken L, Gabilondo I, et al. Treatment and prognostic factors for long-term outcome in patients with anti-NMDA receptor encephalitis: an observational cohort study. *Lancet Neurol*. 2013;12(2):157-165.
- Gadoth A, Pittock SJ, Dubey D, et al. Expanded phenotypes and outcomes among 256 LGII/CASPR2-IgG-positive patients. *Ann Neurol*. 2017;82(1):79-92.
- Irani SR, Michell AW, Lang B, et al. Faciobrachial dystonic seizures precede LGII antibody limbic encephalitis. *Ann Neurol*. 2011;69(5):892-900.
- van Sonderen A, Petit-Pedrol M, Dalmau J, Titulaer MJ. The value of LGII, Caspr2 and voltage-gated potassium channel antibodies in encephalitis. *Nat Rev Neurol*. 2017;13(5):290-301.
- Petit-Pedrol M, Armangue T, Peng X, et al. Encephalitis with refractory seizures, status epilepticus, and antibodies to the GABA(A) receptor: a case series, characterisation of the antigen, and analysis of the effects of antibodies. *Lancet Neurol*. 2014;13(3):276-286.
- Spatola M, Petit-Pedrol M, Simabukuro MM, et al. Investigations in GABAA receptor antibody-associated encephalitis. *Neurology*. 2017;88(11):1012-1020.
- O'Connor K, Waters P, Komorowski L, et al. GABAA receptor autoimmunity: a multicenter experience. *Neurol Neuroimmunol Neuroinflamm*. 2019;6(3):e552.
- Guo CY, Gelfand JM, Geschwind MD. Anti-gamma-aminobutyric acid receptor type A encephalitis: a review. *Curr Opin Neurol*. 2020;33(3):372-380.
- Pettingill P, Kramer HB, Coebergh JA, et al. Antibodies to GABA(A) receptor alpha 1 and gamma 2 subunits clinical and serologic characterization. *Neurology*. 2015;84(12):1233-1241.
- Ohkawa T, Satake SI, Yokoi N, et al. Identification and characterization of GABA(A) receptor autoantibodies in autoimmune encephalitis. *J Neurosci*. 2014;34(24):8151-8163.
- Smith SM. Fast robust automated brain extraction. *Hum Brain Mapp*. 2002;17(3):143-155.
- Yushkevich PA, Piven J, Hazlett HC, et al. User-guided 3D active contour segmentation of anatomical structures: significantly improved efficiency and reliability. *Neuroimage*. 2006;31(3):1116-1128.
- Matthews L, Marasco R, Jenkinson M, et al. Distinction of seropositive NMO spectrum disorder and MS brain lesion distribution. *Neurology*. 2013;80(14):1330-1337.
- Yang L, Li H, Xia W, et al. Quantitative brain lesion distribution may distinguish MOG-ab and AQP4-ab neuromyelitis optica spectrum disorders. *Eur Radiol*. 2020;30(3):1470-1479.
- Giorgio A, Battaglini M, Gentile G, et al. Mapping the progressive treatment-related reduction of active MRI lesions in multiple sclerosis. *Front Neurol*. 2020;11:585296.
- Avants BB, Tustison NJ, Song G, Cook PA, Klein A, Gee JC. A reproducible evaluation of ANTs similarity metric performance in brain image registration. *Neuroimage*. 2011;54(3):2033-2044.
- French L, Paus T. A FreeSurfer view of the cortical transcriptome generated from the Allen Human Brain Atlas. *Front Neurosci*. 2015;9:323.
- Hawrylycz MJ, Lein ES, Guillozet-Bongaarts AL, et al. An anatomically comprehensive atlas of the adult human brain transcriptome. *Nature*. 2012;489(7416):391-399.
- Laurido-Soto O, Brier MR, Simon LE, McCullough A, Bucelli RC, Day GS. Patient characteristics and outcome associations in AMPA receptor encephalitis. *J Neurol*. 2019;266(2):450-460.
- Simabukuro MM, Petit-Pedrol M, Castro LH, et al. GABAA receptor and LGII antibody encephalitis in a patient with thymoma. *Neurol Neuroimmunol Neuroinflamm*. 2015;2(2):e73.
- Vacchiano V, Giannoccaro MP, Napolitano RP, et al. Combined brain positron emission tomography/magnetic resonance imaging in GABAA receptor encephalitis. *Eur J Neurol*. 2019;26(10):e88-e89.
- Fujimori J, Takai Y, Nakashima I, et al. Bilateral frontal cortex encephalitis and paraparesis in a patient with anti-MOG antibodies. *J Neurol Neurosurg Psychiatry*. 2017;88(6):534-536.
- Kamada T, Miura S, Harada M, et al. Bilateral cingulate cortices lesions in two autoantibodies directed against MOG (MOG-Ab)-positive patients. *Mult Scler Relat Disord*. 2019;29:108-110.

# Neurology<sup>®</sup> Neuroimmunology & Neuroinflammation

## **MRI Characteristics of Autoimmune Encephalitis With Autoantibodies to GABAA Receptor: A Case Series**

Bo Deng, Mengfei Cai, Yue Qiu, et al.  
*Neurol Neuroimmunol Neuroinflamm* 2022;9;  
DOI 10.1212/NXI.0000000000001158

**This information is current as of March 25, 2022**

*Neurol Neuroimmunol Neuroinflamm* is an official journal of the American Academy of Neurology. Published since April 2014, it is an open-access, online-only, continuous publication journal. Copyright © 2022 The Author(s). Published by Wolters Kluwer Health, Inc. on behalf of the American Academy of Neurology.. All rights reserved. Online ISSN: 2332-7812.



<b>Updated Information &amp; Services</b>	including high resolution figures, can be found at: <a href="http://nn.neurology.org/content/9/3/e1158.full.html">http://nn.neurology.org/content/9/3/e1158.full.html</a>
<b>References</b>	This article cites 25 articles, 4 of which you can access for free at: <a href="http://nn.neurology.org/content/9/3/e1158.full.html##ref-list-1">http://nn.neurology.org/content/9/3/e1158.full.html##ref-list-1</a>
<b>Citations</b>	This article has been cited by 1 HighWire-hosted articles: <a href="http://nn.neurology.org/content/9/3/e1158.full.html##otherarticles">http://nn.neurology.org/content/9/3/e1158.full.html##otherarticles</a>
<b>Subspecialty Collections</b>	This article, along with others on similar topics, appears in the following collection(s): <b>Autoimmune diseases</b> <a href="http://nn.neurology.org/cgi/collection/autoimmune_diseases">http://nn.neurology.org/cgi/collection/autoimmune_diseases</a> <b>Encephalitis</b> <a href="http://nn.neurology.org/cgi/collection/encephalitis">http://nn.neurology.org/cgi/collection/encephalitis</a> <b>MRI</b> <a href="http://nn.neurology.org/cgi/collection/mri">http://nn.neurology.org/cgi/collection/mri</a>
<b>Errata</b>	An erratum has been published regarding this article. Please see <a href="#">next page</a> or: <a href="/content/9/6/e200040.full.pdf">/content/9/6/e200040.full.pdf</a>
<b>Permissions &amp; Licensing</b>	Information about reproducing this article in parts (figures,tables) or in its entirety can be found online at: <a href="http://nn.neurology.org/misc/about.xhtml#permissions">http://nn.neurology.org/misc/about.xhtml#permissions</a>
<b>Reprints</b>	Information about ordering reprints can be found online: <a href="http://nn.neurology.org/misc/addir.xhtml#reprintsus">http://nn.neurology.org/misc/addir.xhtml#reprintsus</a>

*Neurol Neuroimmunol Neuroinflamm* is an official journal of the American Academy of Neurology. Published since April 2014, it is an open-access, online-only, continuous publication journal. Copyright Copyright © 2022 The Author(s). Published by Wolters Kluwer Health, Inc. on behalf of the American Academy of Neurology.. All rights reserved. Online ISSN: 2332-7812.



## MRI Characteristics of Autoimmune Encephalitis With Autoantibodies to GABAA Receptor: A Case Series

*Neurol Neuroimmunol Neuroinflamm* 2022;9:e200040. doi:10.1212/NXI.0000000000200040

In the Research Article “MRI Characteristics of Autoimmune Encephalitis With Autoantibodies to GABAA Receptor: A Case Series” by Deng et al.<sup>1</sup>, it should be noted that Shuguang Chu and Xiangjun Chen are co–senior authors. The authors regret the omission.

### REFERENCE

1. Deng B, Cai M, Qiu Y, et al. MRI characteristics of autoimmune encephalitis with autoantibodies to GABAA receptor: a case series. *Neurol Neuroimmunol Neuroinflamm*. 2022;9(3):e1158.